

Shockingly bright [OI] 63 μm lines from the supernova remnants W44 and 3C391^{*}

William T. Reach¹ and Jeonghee Rho²

¹ Institut d'Astrophysique Spatiale, Bât. 121, Université Paris XI, F-91405 Orsay Cedex, France

² Service d'Astrophysique, CEA, DSM, DAPNIA, Centre d'Etudes de Saclay, F-91191 Gif-sur-Yvette Cedex, France

Received 4 July 1996 / Accepted 31 July 1996

Abstract. The brightness of the [OI] 63 μm line was measured for the supernova remnants W44 and 3C391 with the *ISO* Long-Wavelength Spectrometer. Bright lines, $\sim 0.3 - 1.4 \times 10^{-3}$ erg cm⁻² sr⁻¹, were detected in the 20 positions observed toward both remnants. The lines are brightest at the edges of the remnants, but they are also bright towards the remnant interior. Continuum emission from collisionally-heated dust is detected, and the dust temperature is 50 K for 3C391. Comparison to theoretical models that predict the [OI] line brightness suggests pre-shock densities $> 10^3$ cm⁻³ and ram pressures of order 10^{-7} dyne cm⁻², as might occur for a supernova blast wave interacting with a molecular cloud.

Key words: ISM: supernova remnants – infrared: interstellar: lines – infrared: interstellar: continuum – ISM: individual objects: 3C391 – ISM: individual objects: W44

1. Introduction

When a massive star ends its life in a supernova explosion (Type II), it often does so in the vicinity of molecular clouds—either that from which it originated or others nearby. The passage of strong shocks into dense gas significantly affects the evolution of both supernova remnant and cloud. The radio shell of 3C391 corresponds in detail to the edge of a large molecular cloud (Wilner et al. 1996), suggesting that the supernova explosion occurred near the edge of the cloud, which has virtually stopped the expansion in this direction. 3C391 and W44, two examples of composite remnants with shell-like radio emission and center-filled X-ray emission, are evidently the result of supernovae near or inside molecular clouds. For W44, there is an

associated pulsar (Wolszczan et al. 1991), so it was a Type II supernova, and there are nearby molecular clouds. For both 3C391 and W44, shock-excited OH masers have been recently discovered (Frail et al. 1996), confirming the interaction between the remnants and molecular clouds.

The interaction of a shock front with the interstellar medium (ISM) produces a variety of bright lines from collisionally excited atoms, ions, and molecules, which in principle will allow us to diagnose the physical conditions. However, the most important lines are obscured by the Earth's atmosphere. The post-shock gas cools through lines from vibrationally excited of H₂ and fine structure and metastable lines that of [OI] (Hollenbach & McKee 1989, Draine et al. 1980). For only one remnant (IC443) have the vibrationally excited H₂ and [OI] 63 μm lines been observed—the latter only in a few positions, using the recently decommissioned NASA Kuiper Airborne Observatory (Burton et al. 1990). In this Letter, we report new observations of the [OI] 63 μm line made with the Long-Wavelength Spectrometer (LWS; Clegg et al. 1996), which is part of the recently-launched Infrared Space Observatory (*ISO*; Kessler et al. 1996).

2. Observations

The observations reported here are *ISO* LWS grating scans of the [OI] 63 μm line. The intensity was measured in each of 20 grating steps, with an interval of 0.0725 μm (1/4 of the grating resolution), such that 63.1837 μm was centered in detector SW3. For each spectrum, a total of 9 grating scans were performed, alternating backward and forward. As a consequence of the LWS design, the brightness was measured in all 10 detectors, centered on wavelengths 43.1, 53.2, 63.2, 72.8, 82.1, 96.5, 116.2, 136.0, 154.9, and 172.6 μm . Thus the [OI] line and the continuum in 10 narrow wavebands were measured simultaneously.

The remnants are much larger than the beamsizes (80'' FWHM), so we made one-dimensional cuts through the regions where there was evidence for an interaction between the supernova shock and a molecular cloud. For W44 (see Fig. 1), we made two cuts, one along the bright radio ridge, and the other perpendicular to it. The spacing between spectra was 180'' for

Send offprint requests to: W.T. Reach, reach@ias.fr

^{*} Based on observations with the Infrared Space Observatory (ISO). ISO is an ESA project with instruments funded by ESA Member States (especially the PI countries: France, Germany, the Netherlands and the United Kingdom) and with the participation of ISAS and NASA.

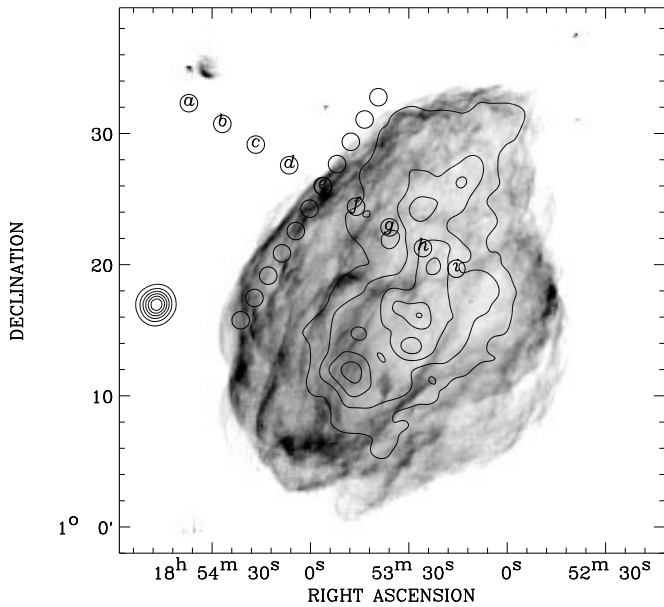


Fig. 1. Radio (greyscale; Jones et al. 1993) and X-ray (contour; Rho et al. 1994) composite map of W44. While the radio emission is shell-like, the X-ray emission is center-filled. The locations of the new *ISO* observations superposed as circles labeled (a) to (i). The diameters of the circles are equal to the *ISO* LWS beam size (FWHM).

the perpendicular cut (shown in Fig. 2) and $120''$ for the cut along the ridge (not shown). Both scans pass through the position of an OH maser (Frail et al. 1996). These observations were performed sequentially, and the brightnesses agree well in the common position. The perpendicular cut extends well outside of the remnant, and the cut along the ridge has one point outside the remnant. For 3C391 (see Fig. 3), we made one cut with a spacing of $50''$, passing from the pre-shock molecular cloud, through the position of an OH maser (Frail et al. 1996), and into the more diffuse part of the remnant that has X-rays but little radio emission (Fig. 4).

3. Results

The [OI] line was detected in every spectrum, both inside and outside the remnant. For each spectrum, we fitted a combination of a Gaussian and a straight line. Results for the 9-position cut perpendicular to the W44 shock are shown in Figure 2, and for 4 of the 9 positions toward 3C391 in Figure 4. Line emission is clearly detected from both the remnant *and* from its surroundings. The emission outside the remnant is due to the pre-shock molecular cloud and some unrelated diffuse emission from the Galaxy. The brightness jumps by a factor of 12 at the position of the W44 radio shell. The [OI] line just outside 3C391 is brighter than that outside W44, probably because the diffuse emission from the Galaxy is brighter at the lower latitude of 3C391.

The spectral lines are all unresolved at the grating resolution (1400 km s^{-1}), but the centroid of the lines varies somewhat

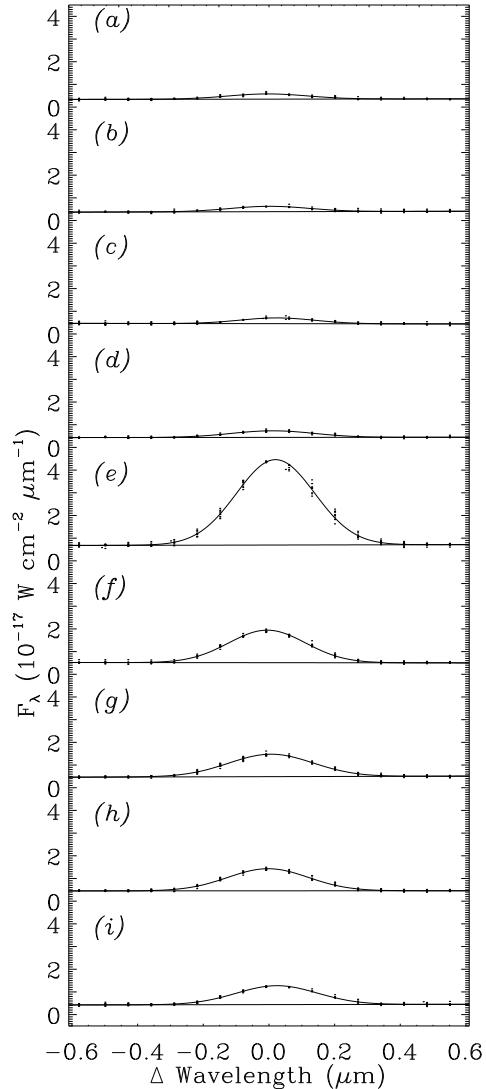


Fig. 2. Nine [OI] line spectra towards W44. The angular between spectra is $180''$. For each line of sight, the grating was stepped back and forth through 20 steps, and each individual measurement is shown as a dot. The locations of the spectra on the radio and X-ray maps in the previous Figure. From the top to the bottom, the regions sampled are outside the remnant (a–d), the radio shell and OH maser (e), and the remnant interior (f–i).

from position to position in 3C391: the shift from one side of the remnant to the other is $\sim 400 \text{ km s}^{-1}$. The preliminary wavelength calibration of the LWS grating has an r.m.s. dispersion of $0.015 \mu\text{m}$, which corresponds to 71 km s^{-1} , smaller than the shifts we observe. At the position in 3C391 closest to the OH maser, the [OI] centroid is -100 km s^{-1} , which is significantly different from the velocity of the maser, $+106 \text{ km s}^{-1}$ (Frail et al. 1996), but at our resolution emission (and absorption) could arise within $\pm 400 \text{ km s}^{-1}$ without substantially broadening the line. Furthermore the rather narrow range of physical conditions required to produce the OH masers may not

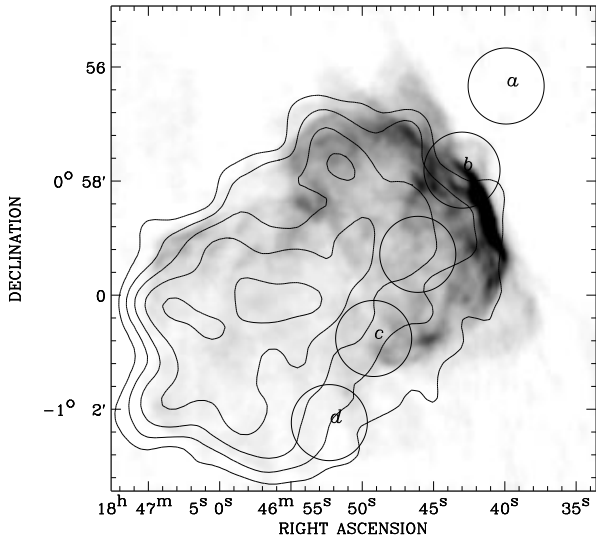


Fig. 3. Radio (greyscale; Reynolds & Moffett 1993) and X-ray (contour; Rho & Petre 1996) composite map of 3C391. The circles labeled (a) to (d) correspond to the locations of the *ISO* spectra shown in the next Figure.

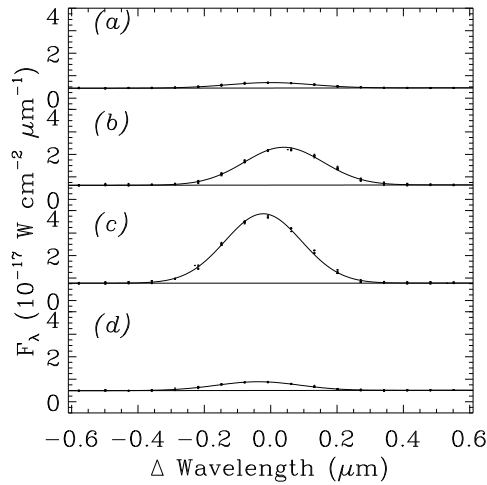


Fig. 4. Four [OI] line spectra towards 3C391. The locations of the spectra on the radio and X-ray maps in the previous Figure. The spectra progress from the pre-shock molecular cloud (a) to the first crossing of the radio shell (b), to the second crossing of the radio shell at the location of the OH maser (c), and back out of the remnant (d).

be those that produce the brightest [OI] emission, so detailed agreement is not expected.

No spectral lines other than [OI] were found in the limited wavelength ranges observed by the 10 detectors; upper limits for some lines toward the peak of 3C391 are $I(\text{CO}[19-18]) < 5 \times 10^{-4}$, $I(\text{CO}[32-31]) < 5 \times 10^{-5}$, and $I(\text{H}10\alpha) < 7 \times 10^{-5}$ $\text{erg cm}^{-2} \text{sr}^{-1}$. For comparison the [OI] 63.2 μm line is 1.4×10^{-3} $\text{erg cm}^{-2} \text{sr}^{-1}$ at this position.

Continuum emission is detected in every detector, from 42.5 to 174 μm . At every position, the continuum peaks around 150

μm , characteristic of dust heated by the diffuse interstellar radiation field. The continuum brightness at long wavelengths shows no correlation with the [OI] line brightness nor with the radio or X-ray brightness, so it is dominated by dust in pre-shock and unrelated clouds. However, at 63 and 73 μm at least, the continuum is higher toward the remnant than outside. For 3C391, the continuum brightness is well correlated with the [OI] line brightness; the correlation coefficient > 0.9 at 53–96 μm . For W44, there is a continuum peak at the position of the [OI] peak, but there is no detailed correlation. The continuum spectrum of the OH maser, after subtracting the off-remnant brightness, has a color temperature 50 ± 10 K (for a $\nu^{1.5}$ emissivity), and surface brightness at 72.8 μm of ~ 150 MJy sr^{-1} , some 30% of the total surface brightness at this position. The color temperature is very similar to that obtained from *IRAS* observations (Arendt 1989). While the line-to-continuum ratio is still rather uncertain with the initial calibration for extended emission, we estimate that the [OI] line would contribute some 10–20% of the brightness averaged over the *IRAS* 60 μm passband.

4. Interpretation

The strong enhancement in [OI] brightness at the edges of the remnants clearly indicates that the emission is from shocked gas. Further, the fact that the [OI] line brightness peaks at the locations of the shock-excited OH masers, together with circumstantial evidence from the distribution of molecular gas around the remnants, suggests the shocks are propagating into molecular clouds. If the [OI] emission extends across the surfaces of the remnants, as appears likely, then the luminosity is $\sim 10^3 L_{\odot}$. A similar (or larger) luminosity arises from the dust continuum. Such an energy loss would add up to the entire supernova energy in $\sim 10^6$ yr. The ages of both remnants considered here have been estimated to be $\sim 10^4$ yr, based on the spin-down age of a pulsar believed to be the W44 progenitor and the X-ray brightness and radius of both remnants. Thus on a global energetic argument, inasmuch as the [OI] 63 μm line and dust continuum are two of the main sources of radiative energy loss behind the shock front, both remnants are in the adiabatic phase of their evolution, and will become radiative when they age by a factor of a few.

To better understand the physical conditions of [OI] emitting regions, we compared theoretical predictions for plane-parallel shock fronts to an [OI] line brightness of 10^{-3} $\text{erg cm}^{-2} \text{sr}^{-1}$. This is the peak surface brightness for W44 and 2/3 of the peak for 3C391. Because the real shock fronts can be beam diluted or tilted with respect to the line of sight, and because there could be multiple shock fronts in each beam, we can only use the models as a rough guide to the plausible physical conditions of the emitting regions. The model of Hollenbach & McKee (1989) applies to fast, dissociative shocks assumed to have a jump (J) discontinuity in the hydrodynamic variables. They find that the [OI] line brightness is roughly proportional to the product of density n_c and shock velocity v_c , which for our line brightness would be $n_c v_c \sim 10^5 \text{ cm}^{-3} \text{ km s}^{-1}$. The model with $n_c = 10^3 \text{ cm}^{-3}$ and $v_c = 100 \text{ km s}^{-1}$ works, but higher-

density models would require shock velocities too low for the assumption of a jump shock. The model of Draine, Roberge, & Dalgarno (1980) applies to slower shocks, with a continuous (C) variation of hydrodynamic variables. [OI] lines in the range of observed brightnesses are predicted for $n_c \sim 10^5 \text{ cm}^{-3}$ and $v_c \sim 10 \text{ km s}^{-1}$. The very high pre-shock densities required to produce the observed [OI] lines are clearly further evidence that the shocks are propagating into molecular clouds. The C-shock and J-shock models predict drastically different brightnesses for other spectral lines, which will allow them to be observationally distinguished now that the [OI] line brightnesses are known.

The shock models that predict the brightness of the [OI] lines for W44 and 3C391 have ram pressures $\rho_c v_c^2 \sim 2 \times 10^{-7} \text{ dyne cm}^{-2}$. This is significantly higher than the thermal pressure of the plasma in the remnant interior: $2n_e k T_e \sim 10^{-9} \text{ dyne cm}^{-2}$ based on the X-ray emission measure and temperature (Rho et al. 1994, Rho & Petre 1996). For an adiabatic remnant, the product of pressure and volume remains constant, and the pressure in the [OI] emitting regions would be higher than the present ram pressure by the inferred amount if the shock hit the dense region when it was $\sim 1/4$ of its present size. This explanation is unlikely to account for the high inferred pressures, however, because we observe bright [OI] lines all the way to the present edges of the remnants, as delineated by the radio continuum shells.

If the supernova occurred near the surface of a molecular cloud, the pre-shock density would be high (n_c) in one direction and low (n_o) in the other. If we apply the Sedov-Taylor solution separately to the shocks propagating into the two different regions, then the ratio of the pressures in the two regions is $p_c/p_o = (n_c/n_o)^{3/5}$. For $n_o \sim 1 \text{ cm}^{-3}$ and $n_c \sim 10^3 \text{ cm}^{-3}$, the pressure of the shock into the molecular cloud is higher than that into the more diffuse medium by about the factor we inferred from comparing the [OI] and X-ray observations. A pressure difference within the remnant is possible, because the sound-crossing time ($\sim 10^5 \text{ yr}$ based on the temperature of the X-ray emitting plasma) is longer than the age of the remnant. The remnant may already contain radiative shocks where it is impacting denser portions of the molecular cloud, though on a global scale the remnant remains adiabatic. This scenario is especially attractive for 3C391, with its clear breakout radio morphology (thin radio shell well-aligned with the edge of a CO cloud) and X-rays much brighter on the lower-density side.

An additional possibility for the origin of some of the [OI] brightness is dense clumps embedded in a lower-density intercloud medium. The shock front through the intercloud gas rapidly passes the clump, which continues to be shocked as well as evaporating inside the remnant. In this case a higher pressure for the shock into the denser gas is also possible (McKee et al. 1987), but the pressure enhancement is large only if the cloud shock began when the remnant was significantly smaller than now, so bright lines at the edge of the remnant are not easily explained. This scenario could apply to the [OI] line brightness observed toward the center of W44.

Acknowledgements. We thank Dale Frail and Miller Goss for providing positions of the OH masers in advance of publication. WTR thanks Pierre Cox for help in understanding the LWS calibration. The observations reported here are part of the *ISO* open time granted to U.S. astronomers.

References

- Arendt, R. G. 1989, *ApJS*, 70, 1
 Burton, M. G., Hollenbach, D. J., Haas, M. R., Erickson, E. F. 1990, *ApJ*, 355, 197
 Clegg, P. E. 1996, this issue
 Draine, B. T., Roberge, W. G., Dalgarno, A. 1983, *ApJ*, 264, 485
 Frail, D. A., Goss, W. M., Reynoso, E. M., Giacani, E. B., Green, A. J., Otrupceck, R. 1996, *AJ*, 111, 1651
 Hollenbach, D. J., McKee, C. F. 1989, *ApJ*, 342, 306
 Jones, L. R., Smith, A., Angellini, L. 1993, *MNRAS*, 265, 631
 Kessler, M. et al. 1996, this issue
 McKee, C. F., Hollenbach, D. J., Seab, C. G., Tielens, A. G. G. M. 1987, *ApJ*, 318, 674
 Reynolds, S. P., Moffett, D. A. 1993, *AJ*, 105, 222
 Rho, J.-H., Petre, R., 1996, *ApJ*, 467, 698
 Rho, J.-H., Petre, R., Schlegel, E. M., Hester, J. J. 1994, *ApJ*, 430, 757
 Wilner, D., Reynolds, S. P., Moffett, D. A. 1996, *BAAS*, 28, 948
 Wolszczan, A., Cordes, J. M., Dewey, R. J. 1991, *ApJL*, 372, L99